Title: ENaC activity in collecting ducts modulates NCC in cirrhotic mice.

Authors: Mordasini D, Loffing-Cueni D, Loffing J, Beatrice R, Maillard MP, Hummler E, Burnier M, Escher G, Vogt B

Journal: Pflugers Archiv : European journal of physiology

Year: 2015 Dec

Volume: 467

Issue: 12

Pages: 2529-39

DOI: 10.1007/s00424-015-1711-7

David Mordasini[1], Dominique Loffing-Cueni[4], Johannes Loffing[4], Rohrbach Beatrice[1], Marc P. Maillard[2], Edith Hummler[3], Michel Burnier[2], Geneviève Escher[1*] and Bruno Vogt[1*]

ENaC activity in collecting ducts modulates NCC in cirrhotic mice

[1]Department of Nephrology, Hypertension and Clinical Pharmacology, Inselspital, Bern University Hospital, Department of Clinical Research, University of Bern, Switzerland; [2]Service of Nephrology and Hypertension, CHUV, Rue du Bugnon 17, CH-1005 Lausanne, Switzerland; [3]University of Lausanne, Department of Pharmacology and Toxicology, Rue du Bugnon 27, CH-1005 Lausanne; [4]University of Zurich, Institute of Anatomy, University of Zurich, Zurich, Switzerland

*Contributed equally to the work

Correspondence:

David Mordasini, PhD
Universitätsklinik für Nephrologie, Hypertonie und Klinische Pharmakologie, Inselspital
CH-3010 Bern, Schweiz
Phone: +41 31 632 9747
Fax: +41 31 632 9444
E-Mail: david.mordasini@dkf.unibe.ch

ABSTRACT:

Cirrhosis is a frequent and severe disease, complicated by renal sodium retention leading to ascites and oedema. A better understanding of the complex mechanisms responsible for renal sodium handling could improve clinical management of sodium retention. Our aim was to determine the importance of the amiloride-sensitive epithelial sodium channel (ENaC) in collecting ducts in compensate and decompensate cirrhosis.

Bile duct ligation was performed in control mice (CTL) and collecting duct specific αENaC knock-out mice (KO), and ascites development, aldosterone plasma concentration, urinary sodium/potassium ratio and sodium transporter expression were compared.

Disruption of ENaC in cortical collecting ducts (CCDs) did not alter ascites development, urinary sodium/potassium ratio, plasma aldosterone concentrations, or Na,K-ATPase abundance in CCDs. Total αENaC abundance in whole kidney increased in cirrhotic mice of both genotypes and cleaved forms of α and γ ENaC increased only in ascitic mice of both genotypes. The sodium chloride cotransporter (NCC) abundance was lower in non ascitic KO, compared to non ascitic CTL, and increased when ascites appeared.

In ascitic mice, the lack of αENaC in CDs induced an upregulation of total ENaC and NCC and correlated with the cleavage of ENaC subunits. This revealed compensatory mechanisms which could also take place when treating the patients with diuretics. These compensatory mechanisms should be considered for future development of therapeutic strategies.

KEYWORDS: Ascites, aldosterone, cirrhosis, cortical collecting ducts, ENaC, NCC

INTRODUCTION

Cirrhosis is a frequent and severe disease, complicated by renal sodium retention leading to ascites and oedema. The development of the disease starts with damages to the liver architecture causing an increase of intrahepatic resistance and leading to portal hypertension. The latter is known to stimulate the production of nitric oxide, which in turn induces a peripheral arterial vasodilatation and causes intravascular volume insufficiency. This triggers mechanisms of sodium and water conservation through the renin-angiotensin-system, the sympathetic nervous system and the vasopressin pathway. It is hypothesized that an inadequate stimulation of these pathways leads to renal sodium retention which will favour ascites accumulation [13,25]. However, cellular and molecular mechanisms responsible for unbalanced renal sodium transport are incompletely understood.

We showed previously, that bile duct-ligated mice developed ascites concomitantly to Na,K-ATPase stimulation in cortical collecting ducts exclusively [1]. Underlining the role of the aldosterone sensitive distal nephron in ascites development, studies performed with rats showed an increased apical targeting of ENaC in ascitic animals [20,21]. In order to investigate the role of collecting ducts (CDs) in cirrhosis-induced sodium retention, we used a transgenic mouse model with a CD-specific inactivation of the amiloride sensitive sodium channel (ENaC) [29], which is crucial for regulated renal sodium reabsorption. Rubera *et al*. showed that mice with disruption of αENaC in CDs were still able to maintain sodium and potassium balance, even when challenged by salt restriction, water deprivation, or potassium loading [29]. Our hypothesis was that in pathological conditions, such as cirrhosis, CD function may become of importance.

The aim of the present study was to determine the importance of ENaC in CDs using the bile duct ligation-induced cirrhosis mouse model. We investigated ascites development, plasma aldosterone concentrations, urinary sodium and potassium excretion, as well as the expression of ENaC subunits, sodium chloride co-transporter (NCC) and Na,K-ATPase in control (CTL) and αENaC KO (KO) mice.

SUBJECTS AND METHODS

Animals

Animal studies were approved by the Veterinary Service of the Canton de Vaud, Switzerland. Experiments were performed on adult CTL (*Scnn1a*$^{lox/lox}$) and αENaC KO (*Hoxb7::cre/scnn1a*$^{lox/lox}$) mice.

Bile duct ligation

The bile duct ligation was performed under anaesthesia mediated by isoflurane inhalation (57 CTL and 53 KO). A ventral incision was made; ligatures were tightened around the bile duct and the segment in between excised. The same procedure was performed in SHAM-operated mice (12 CTL and 10 KO) except that no ligatures were tightened. After ligation, abdominal muscles were sutured and skin closed with *Michel's* suture clips. Mice were observed daily and received paracetamol (200 mg·kg^{-1}·day^{-1}) in drinking water for 2 days following surgery.

Ascites quantitation

Ascites development was monitored by body weight measurement. The mice with or without ascites were determined *a posteriori* at the time of sacrifice; mice with ascites at the time of sacrifice were considered as mice BDL+ even ascites was not present yet. The rate of ascites accumulation was estimated by the calculation of bodyweight difference between a measurement and the previous one.

Plasma aldosterone concentrations

Plasma aldosterone concentrations were measured by RIA (Coat-a-Count; Diagnostics Products Inc.).

Immunostaining

Kidneys of anesthetized mice were fixed for 5 minutes with 3% PFA in phosphate buffer by retrograde perfusion via the abdominal aorta [22]. Kidneys were cut in thin sections, frozen in liquid propane and stored at -80°C until further analysis. Immunohistochemistry was performed on 4 µm cryosections. Sections were blocked with 10% normal goat serum and subsequently incubated over night at 4°C with the primary antibodies (N-ter αENaC 1/5000 [32]); followed by a Cy3-conjugated donkey anti-rabbit IgG (Jackson Immuno Research Laboratories) diluted 1/1000. The sections were analysed by a fluorescence microscope (Leica). Pictures were taken with a CCD-camera and processed with Adobe Photoshop and Microsoft PowerPoint softwares.

Urine collection

Mice were installed into restraining tube, every 3 to 4 days from 8:00 am to 11:00 am, for urine collection. Urinary sodium and potassium were measured by flame photometry (IL943, Instrumentation Laboratory).

Microdissection of renal tubules

The left kidney was perfused with a liberase containing solution (liberase TM 33 µg/ml from Roche in DMEM/F-12, 1:1; Invitrogen). Pyramids cut along the corticomedullary axis were incubated at 30°C for 40 min in perfusion medium. Tubules were isolated in ice-cold DMEM/F-12 supplemented with 0.05% BSA without liberase. Tubules were transferred into 96 well plates and photographed. The total length of tubules was measured using Image J [31].

Na,K-ATPase Assay

Na,K-ATPase activity was determined as previously described [5]. Total ATPase activity was determined in a solution containing 50 mM NaCl, 5 mM KCl, 10 mM $MgCl_2$, 1 mM EGTA, 100 mM Tris-HCl, 10 mM Na_2ATP, and 8 nCi/µl of ATP [γ-^{32}P] (10 Ci/mmol, 2 mCi/ml, Perkin Elmer: BLU002250UC) at pH 7.4. For Na^+, K^+-independent ATPase activity measurements, NaCl and KCl were omitted, Tris-HCl was 150 mM, and 2 mM ouabain was added. Na,K-ATPase activity was taken as the difference between total and Na^+, K^+-independent ATPase activities and expressed as the mean in pmole·mm^{-1}·$hour^{-1}$ of n measurements.

122
123 SDS-PAGE and Immunoblotting
124
125 Kidneys were homogenized using a Dounce tissue grinder and membrane proteins extracted in presence of
126 protease and phosphatase inhibitors (No. 78440, Pierce) according to the manufacturer protocol (MEM Per Plus
127 Kit No. 89842, Pierce). Protein concentration was quantified using the BCA protein assay kit (No. 23225,
128 Pierce). Ten microgram were separated by SDS-PAGE, then transferred on nitrocellulose membrane and stained
129 with Ponceau red before immunodetection. Nitrocellulose membranes were incubated with primary antibodies
130 detecting, αENaC (1/10000) [32], βENaC (1/10000) [33] and γENaC (1/10000) [33] and NCC (1/10000) [32].
131 Immunoblots were scanned using the Molecular Imager Chemidoc XRS+ (Biorad). Relative quantification was
132 obtained by dividing the densitometric values of the proteins of interest by the densitometric values obtained
133 with Ponceau red staining for the corresponding lane.
134
135 Total RNA extraction and qPCR
136
137 Total RNA was extracted from kidneys with Trizol according manufacturer's protocol (Life Technologies).
138 Reverse transcription was performed on 1 µg of total RNA with the ImProm-II™ Reverse Transcription System
139 (Promega). Relative abundances of transcripts were calculated after qPCR amplification. Primers and probes
140 number - corresponding to the Universal ProbeLibrary (Roche) - targeting transcripts of interest, described in
141 **table 1**, were designed using ProbeFinder software (Roche).
142
143 Statistics
144
145 Results are expressed as means ± SEM from several animals. To determine statistically significant differences,
146 Student t-test or 1- or 2-way analysis of variance were used, followed by Bonferroni's tests for multiple
147 comparisons.
148
149 RESULTS
150
151 Control and collecting duct alpha ENaC KO mice develop ascites
152
153 The presence of ascites was a prerequisite to identify cirrhotic mice with sodium retention. Ascites development
154 was indirectly estimated by body weight measurement (**Fig. 1A and B**). Around ten days after BDL, 30% of
155 CTL (17 out of 57) and 36% of KO (18 out of 53) of bile duct-ligated mice rapidly gained weight due to ascites
156 accumulation (BDL+). Mice were sacrificed when ascites was observed for several consecutive days. The
157 proportion of mice developing ascites and their survival rate after bile duct ligation were not affected by the
158 genotype (**Fig. 1C**). Ascites accumulated at 1 ml per day and its volume reached about 10 ml at the time of
159 sacrifice (**Fig. 1D**). Mice which did not gain weight (BDL-) over a period of 20 to 30 days after BDL were
160 sacrificed and considered to be mice with compensated cirrhosis (BDL-).
161

Immunolocalization confirms αENaC disruption in CDs

Deletion of αENaC along collecting ducts (CDs) of αENaC KO mice was assessed by immunostaining (**Fig. 2**). In CTL mice, αENaC was seen in all principal cells of CDs, independent from the group (SHAM, BDL-, and BDL+). In KO mice, αENaC was absent from CD cells. A very few principal cells with remaining αENaC expression were seen in the initial cortical collecting duct.

Urinary sodium and potassium excretion are similar in CTL and αENaC KO mice

As expected in mice retaining sodium, 2-way analysis of variance with presence of ascites (BDL- vs BDL+) and genotype as a factor revealed a significant reduction of the urinary Na^+/Creatinine as well as Na^+/K^+ ratio in BDL+ ($p = 0.0133$ and $p = 0.0217$ respectively), which was not affected by the genotype (**Fig. 3A**).

Plasma aldosterone concentrations increase in CTL and αENaC KO mice with ascites

Plasma aldosterone concentrations increased independently of genotypes following bile duct ligation. A 2-way analysis of variance of aldosterone plasma concentrations between SHAM, BDL- and BDL+ revealed a significant increase in BDL+ mice (**Fig. 3B**).

ENaC is upregulated in cirrhotic CTL and KO mice

Immunoblots on membrane proteins extracted from kidney homogenates showed increased αENaC abundance in cirrhotic mice (BDL- or BDL+) (**Fig. 4A**). The cleaved form of αENaC appeared as doublets, as previously observed by others [6,10,11]. Statistical analysis of band density quantifications revealed (**Fig. 4B**) an upregulation of total αENaC (full and cleaved forms) in ascitic KO mice and interestingly a greater abundance of αENaC in KO BDL+ vs CTL BDL+ mice. Analysis of the full form showed an increase in BDL- and BDL+ mice, with no differences between genotypes (**Fig. 4C**). An increase of the αENaC cleaved form was observed in ascitic mice; however it was significant only in the KO BDL+ likely due to the variability observed in CTL BDL+ mice. The abundance of the cleaved form was higher in KO BDL+ versus CTL BDL+ ($p < 0.01$) (**Fig. 4D**). The abundance of transcript coding for ENaC (scnn1a) was affected in BDL+ mice independently of genotypes (**Fig. 4E**).

The expression of βENaC subunit (**Fig. 5A**) was not altered in CTL BDL- and CTL BDL+ mice, but was increased in KO BDL- mice (**Fig. 5B**). The abundance of transcript coding for ENaC (scnn1a) was affected in BDL+ mice independently of genotypes (**Fig. 5C**).

Immunoblots showed a higher abundance of the γENaC cleaved form compared to its full form for two CTL BDL+ and KO BDL+ mice and the quasi absence of the γENaC cleaved form in BDL- (**Fig. 6A**). The full γENaC is les abundant in BDL+ than in BDL+ in both genotypes (**Fig. 6C**) while γENaC cleaved form is more abundant in BDL+ than in BDL- mice (**Fig. 6D**). The abundance of transcript coding for ENaC (scnn1a) was affected in BDL+ mice independently of genotypes (**Fig. 6E**).

202 The absence of ENaC activity in collecting ducts does not influence Na,K-ATPase abundance
203
204 Previously used as a marker for sodium reabsorption along renal tubules [1], the Na,K-ATPase activity
205 measurements performed in microdissected tubules at V_{max} reflects the abundance of Na,K-ATPase holoenzyme.
206 In this study, the measurements did not reveal differences between groups (**Fig. 7**).
207
208 Sodium chloride costransporter abundance differs between CTL and KO cirrhotic mice
209
210 Immunoblots on membrane proteins extracted from whole kidney showed reduced NCC abundance in BDL-
211 mice (**Fig. 8A**). Statistical analysis of band density quantification showed a downregulation of NCC in cirrhotic
212 CTL BDL+ and KO BDL- (**Fig. 8B**). Since samples from CTL and KO were loaded on different gels, and thus
213 could not be compared, we did a second electrophoresis to investigate differences between CTL and KO samples
214 in SHAM, BDL- and BDL+ (**Fig. 9A and B**). This revealed a lower NCC abundance in KO BDL- than in CTL
215 BDL-, and a higher abundance in KO BDL+ than in CTL BDL+ mice. The abundance of its transcript was not
216 altered (**Fig. 8C**).
217
218 DISCUSSION
219
220 To our knowledge, this is the first study investigating the mechanisms of sodium retention by bile duct ligation
221 in genetically modified animals. It demonstrated in ascitic mice that the disruption of ENaC and thus a lack of its
222 activity in CDs induced ENaC and NCC in upstream segments. These results on ENaC expression are in line
223 with previous studies demonstrating the importance of ENaC in CNTs for the regulation of sodium reabsorption
224 [9,12,27].
225 The absence of ENaC in CDs did not alter ascites formation. It developed in 30% of CTL and 36% of KO bile
226 duct-ligated mice.
227 The immunohistochemical studies confirmed the disruption of ENaC in CDs of KO mice. Although a very few
228 single cells in cortical collecting ducts escape the cre recombinase mediated inactivation of αENaC, as
229 previously reported [29], we consider it highly unlikely that these few single CD-cells with persistent αENaC
230 expression can account for the absence of differences between CTL and KO mice. It is likely that upstream
231 segments contribute to sodium retention.
232 The urinary Na^+/Creatinine as well as Na^+/K^+ ratios were reduced and plasma aldosterone concentrations
233 increased in BDL+, as observed in humans [4].
234 Western blot analysis showed for both genotypes, an increase of αENaC abundance in BDL- and BDL+, but it
235 also revealed that the cleavage of α and γ subunits was significant only in BDL+ mice, which were retaining
236 sodium. In kidneys, αENaC protein abundance has been shown to be regulated by aldosterone, while βENaC and
237 γENaC not or only weakly [6,26]. Moreover, aldosterone stimulation or low salt diet was shown to induce an
238 apical redistribution of αENaC, βENaC and γENaC [8,10,23,24,26] and cleavage of αENaC and γENaC [6,26].
239 Cleavage of ENaC by exogenous trypsin has been linked to an increase of channel activity [8,28]. Kim *et al*.
240 observed, in ascitic rats, an increased apical targeting of αβγENaC in DCTs, CNTs and CDs, and cleavage of
241 γENaC, without changes of αβγENaC protein abundance [21,20]. Altogether these results showed that in ascitic

animals, α and γ ENaC are cleaved, suggesting an increase in ENaC activity and thus demonstrate its importance for sodium retention. Interestingly, in our study, the αENaC cleaved form was more abundant in KO BDL+ than in CTL BDL+ mice, suggesting insufficient sodium reabsorption and a need to compensate.

We did not observe increase in NCC abundance, although NCC is described as an aldosterone induced protein [19]. The slight decrease in NCC abundance observed in CTL cirrhotic mice was not significant in contrast to what was previously reported [7,14,34]. In BDL- mice NCC protein expression was lower than in CTL, whereas in BDL+ mice, in which sodium retention occurs it was higher in KO than CTL mice and probably reached the same level as in the SHAM operated mice as shown by the results in **fig. 8**. These results suggested compensation by NCC of an insufficient ENaC activity in CDs. The reduced abundance of NCC in non ascitic mice may reflect the aldosterone escape phenomenon, characterized by a downregulation of NCC in presence of high plasma aldosterone concentrations and high salt diet [30]. Conditions which are similar to those encountered by the CTL cirrhotic mice; their plasma aldosterone concentrations are high and their salt intake sufficient. The downregulation of NCC could also be due to an increase in plasma potassium concentration [3]. However, this hypothesis is unlikely since several studies performed in rats reported normal plasma potassium values in cirrhotic animals [14,15,17,18].

In contrast to Ackermann *et al.,* we did not observe any significant up-regulation of the Na,K-ATPase activity in isolated CCDs between SHAM-operated and cirrhotic mice [1]. This difference could be due to the mouse strains used. In the previous study, CD1 mice were used whereas in the actual one, we used 129/Sv x C57BL/6, since they are more prone to develop ascites [2]. Additionally mice were analysed at different time point.

In summary, our study showed that in pathological conditions such as cirrhosis, the amount of sodium reabsorbed through ENaC in CDs is likely not negligible and if not sufficient, NCC upregulation may happen. The upregulation of NCC could explain the blunted natriuretic effect of the amiloride observed in cirrhotic rats treated with amiloride [16].

The control of renal sodium retention and ascites development is not trivial in cirrhotic patients. A better understanding of the mechanisms responsible for renal sodium handling would improve its clinical management. This study illustrates the usability of gene-modified mouse models to dissect the complex mechanisms of sodium retention. It revealed compensation mechanisms which could take place when we downregulate artificially ion transporters, similarly as what is done with diuretics. In conclusion, to develop efficient therapeutic strategies, we have to understand pathways leading to sodium/potassium imbalance and to further consider compensatory mechanisms.

ACKNOWLEDGEMENTS

We thank Professors A Doucet and B Rossier for constructive comments, Dr. H Mistry, Dr. G Crambert and Dr. N Faller for their helpful reading of the manuscript and discussions, and A Tedjani and A Menoud for the technical assistance. We thank Dr. F Schütz (Training and Outreach, Bioinformatics Core Facility, University of Lausanne) for its assistance with statistical analysis.

Financial support: This study was supported by grants from the Swiss National Science Foundation: 31003A_120406 and 31003A_135417 attributed to BV. The laboratory of JL is supported by SNF grant 310030_143929/1.

REFERENCES

1. Ackermann D, Mordasini D, Cheval L, Imbert-Teboul M, Vogt B, Doucet A (2007) Sodium retention and ascites formation in a cholestatic mice model: role of aldosterone and mineralocorticoid receptor? Hepatology 46:173-179. doi:10.1002/hep.21699
2. Alaish SM, Torres M, Ferlito M, Sun CC, De Maio A (2005) The severity of cholestatic injury is modulated by the genetic background. Shock 24:412-416. doi:00024382-200511000-00003 [pii]
3. Ananthanarayanan M, Balasubramanian N, Makishima M, Mangelsdorf DJ, Suchy FJ (2001) Human bile salt export pump promoter is transactivated by the farnesoid X receptor/bile acid receptor. J Biol Chem 276:28857-28865. doi:10.1074/jbc.M011610200
M011610200 [pii]
4. Arroyo V, Bernardi M, Epstein M, Henriksen JH, Schrier RW, Rodes J (1988) Pathophysiology of ascites and functional renal failure in cirrhosis. J Hepatol 6:239-257
5. Doucet A, Katz AI, Morel F (1979) Determination of Na-K-ATPase activity in single segments of the mammalian nephron. Am J Physiol 237:F105-113
6. Ergonul Z, Frindt G, Palmer LG (2006) Regulation of maturation and processing of ENaC subunits in the rat kidney. Am J Physiol Renal Physiol 291:F683-693. doi:00422.2005 [pii]
10.1152/ajprenal.00422.2005
7. Fernandez-Llama P, Jimenez W, Bosch-Marce M, Arroyo V, Nielsen S, Knepper MA (2000) Dysregulation of renal aquaporins and Na-Cl cotransporter in CCl4-induced cirrhosis. Kidney Int 58:216-228. doi:kid156 [pii]
10.1046/j.1523-1755.2000.00156.x
8. Frindt G, Ergonul Z, Palmer LG (2008) Surface expression of epithelial Na channel protein in rat kidney. J Gen Physiol 131:617-627. doi:10.1085/jgp.200809989
jgp.200809989 [pii]
9. Frindt G, Palmer LG (2004) Na channels in the rat connecting tubule. Am J Physiol Renal Physiol 286:F669-674. doi:10.1152/ajprenal.00381.2003
00381.2003 [pii]
10. Frindt G, Palmer LG (2009) Surface expression of sodium channels and transporters in rat kidney: effects of dietary sodium. Am J Physiol Renal Physiol 297:F1249-1255. doi:10.1152/ajprenal.00401.2009
00401.2009 [pii]
11. Frindt G, Palmer LG (2012) Regulation of epithelial Na+ channels by adrenal steroids: mineralocorticoid and glucocorticoid effects. Am J Physiol Renal Physiol 302:F20-26. doi:10.1152/ajprenal.00480.2011
ajprenal.00480.2011 [pii]
12. Fu Y, Gerasimova M, Batz F, Kuczkowski A, Alam Y, Sanders PW, Ronzaud C, Hummler E, Vallon V (2015) PPARgamma agonist-induced fluid retention depends on alphaENaC expression in connecting tubules. Nephron 129:68-74. doi:10.1159/000370254
000370254 [pii]
13. Gines P, Cardenas A, Arroyo V, Rodes J (2004) Management of cirrhosis and ascites. N Engl J Med 350:1646-1654. doi:10.1056/NEJMra035021
350/16/1646 [pii]
14. Graebe M, Brond L, Christensen S, Nielsen S, Olsen NV, Jonassen TE (2004) Chronic nitric oxide synthase inhibition exacerbates renal dysfunction in cirrhotic rats. Am J Physiol Renal Physiol 286:F288-297. doi:10.1152/ajprenal.00089.2003
00089.2003 [pii]
15. Jonassen TE, Brond L, Torp M, Graebe M, Nielsen S, Skott O, Marcussen N, Christensen S (2003) Effects of renal denervation on tubular sodium handling in rats with CBL-induced liver cirrhosis. Am J Physiol Renal Physiol 284:F555-563. doi:10.1152/ajprenal.00258.2002

00258.2002 [pii]
16. Jonassen TE, Heide AM, Janjua NR, Christensen S (2002) Collecting duct function in liver cirrhotic rats with early sodium retention. Acta Physiol Scand 175:237-244. doi:993 [pii]
17. Jonassen TE, Marcussen N, Haugan K, Skyum H, Christensen S, Andreasen F, Petersen JS (1997) Functional and structural changes in the thick ascending limb of Henle's loop in rats with liver cirrhosis. Am J Physiol 273:R568-577
18. Jonassen TE, Nielsen S, Christensen S, Petersen JS (1998) Decreased vasopressin-mediated renal water reabsorption in rats with compensated liver cirrhosis. Am J Physiol 275:F216-225
19. Kim GH, Masilamani S, Turner R, Mitchell C, Wade JB, Knepper MA (1998) The thiazide-sensitive Na-Cl cotransporter is an aldosterone-induced protein. Proc Natl Acad Sci U S A 95:14552-14557
20. Kim SW, Wang W, Nielsen J, Praetorius J, Kwon TH, Knepper MA, Frokiaer J, Nielsen S (2004) Increased expression and apical targeting of renal ENaC subunits in puromycin aminonucleoside-induced nephrotic syndrome in rats. Am J Physiol Renal Physiol 286:F922-935. doi:10.1152/ajprenal.00277.2003
00277.2003 [pii]
21. Kim SW, Wang W, Sassen MC, Choi KC, Han JS, Knepper MA, Jonassen TE, Frokiaer J, Nielsen S (2006) Biphasic changes of epithelial sodium channel abundance and trafficking in common bile duct ligation-induced liver cirrhosis. Kidney Int 69:89-98. doi:5000018 [pii]
10.1038/sj.ki.5000018
22. Loffing J, Loffing-Cueni D, Valderrabano V, Klausli L, Hebert SC, Rossier BC, Hoenderop JG, Bindels RJ, Kaissling B (2001) Distribution of transcellular calcium and sodium transport pathways along mouse distal nephron. Am J Physiol Renal Physiol 281:F1021-1027
23. Loffing J, Pietri L, Aregger F, Bloch-Faure M, Ziegler U, Meneton P, Rossier BC, Kaissling B (2000) Differential subcellular localization of ENaC subunits in mouse kidney in response to high- and low-Na diets. Am J Physiol Renal Physiol 279:F252-258
24. Loffing J, Zecevic M, Feraille E, Kaissling B, Asher C, Rossier BC, Firestone GL, Pearce D, Verrey F (2001) Aldosterone induces rapid apical translocation of ENaC in early portion of renal collecting system: possible role of SGK. Am J Physiol Renal Physiol 280:F675-682
25. Martin PY, Gines P, Schrier RW (1998) Nitric oxide as a mediator of hemodynamic abnormalities and sodium and water retention in cirrhosis. N Engl J Med 339:533-541. doi:10.1056/NEJM199808203390807
26. Masilamani S, Kim GH, Mitchell C, Wade JB, Knepper MA (1999) Aldosterone-mediated regulation of ENaC alpha, beta, and gamma subunit proteins in rat kidney. J Clin Invest 104:R19-23. doi:10.1172/JCI7840
27. Meneton P, Loffing J, Warnock DG (2004) Sodium and potassium handling by the aldosterone-sensitive distal nephron: the pivotal role of the distal and connecting tubule. Am J Physiol Renal Physiol 287:F593-601. doi:10.1152/ajprenal.00454.2003
287/4/F593 [pii]
28. Nesterov V, Dahlmann A, Bertog M, Korbmacher C (2008) Trypsin can activate the epithelial sodium channel (ENaC) in microdissected mouse distal nephron. Am J Physiol Renal Physiol 295:F1052-1062. doi:10.1152/ajprenal.00031.2008
00031.2008 [pii]
29. Rubera I, Loffing J, Palmer LG, Frindt G, Fowler-Jaeger N, Sauter D, Carroll T, McMahon A, Hummler E, Rossier BC (2003) Collecting duct-specific gene inactivation of alphaENaC in the mouse kidney does not impair sodium and potassium balance. J Clin Invest 112:554-565. doi:10.1172/JCI16956
112/4/554 [pii]
30. Sandberg MB, Maunsbach AB, McDonough AA (2006) Redistribution of distal tubule Na+-Cl- cotransporter (NCC) in response to a high-salt diet. Am J Physiol Renal Physiol 291:F503-508. doi:00482.2005 [pii]
10.1152/ajprenal.00482.2005

31. Schneider CA, Rasband WS, Eliceiri KW (2012) NIH Image to ImageJ: 25 years of image analysis. Nat Methods 9:671-675

32. Sorensen MV, Grossmann S, Roesinger M, Gresko N, Todkar AP, Barmettler G, Ziegler U, Odermatt A, Loffing-Cueni D, Loffing J (2013) Rapid dephosphorylation of the renal sodium chloride cotransporter in response to oral potassium intake in mice. Kidney Int 83:811-824. doi:10.1038/ki.2013.14
ki201314 [pii]

33. Wagner CA, Loffing-Cueni D, Yan Q, Schulz N, Fakitsas P, Carrel M, Wang T, Verrey F, Geibel JP, Giebisch G, Hebert SC, Loffing J (2008) Mouse model of type II Bartter's syndrome. II. Altered expression of renal sodium- and water-transporting proteins. Am J Physiol Renal Physiol 294:F1373-1380. doi:10.1152/ajprenal.00613.2007
00613.2007 [pii]

34. Yu Z, Serra A, Sauter D, Loffing J, Ackermann D, Frey FJ, Frey BM, Vogt B (2005) Sodium retention in rats with liver cirrhosis is associated with increased renal abundance of NaCl cotransporter (NCC). Nephrol Dial Transplant 20:1833-1841. doi:gfh916 [pii]
10.1093/ndt/gfh916

405 FIGURES LEGENDS

406

407 **Fig. 1**

408 Evolution of body weight (mean ± SEM) after bile duct ligation of CTL (A) or αENaC KO (B) mice without
409 (BDL-) and with (BDL+) ascites. Fate of mice after bile duct ligation: a 2-sample test for equality of proportions
410 showed no differences between genotypes regarding ascites development (C). Indirect quantification of ascites
411 accumulation rate (mean ± SEM) 6 CTL and 5 KO mice (D).

412

413 **Fig. 2**

414 Renal immunolocalization of αENaC for SHAM, BDL- and BDL+ mice. Collecting ducts (C), proximal tubules
415 (P).

416

417 **Fig. 3**

418 Urinary Na^+, K^+ / Creatinine and Na^+/K^+ ratio and plasma aldosterone concentrations. Urinary Na^+/Creatinine is
419 reduced in BDL+ mice (Fig 3A). 2-way ANOVA, with presence of ascites and genotype as factors; the
420 difference between BDL- and BDL+ is significant ($p = 0.0217$); neither the genotype nor the interaction is
421 significant. Urinary K+/Creatinine is similar between BDL- and BDL+. Urinary Na^+/ K^+ ratio (mean ± SEM) of
422 CTL and KO mice: without ascites, more than 2 weeks after bile duct ligation (BDL-) and with ascites, more
423 than 2 weeks after bile duct ligation (BDL+). 2-way ANOVA, with presence of ascites and genotype as factors;
424 the difference between BDL- and BDL+ is significant ($p = 0.0133$); neither the genotype nor the interaction is
425 significant. Aldosterone plasma concentrations (mean ± SEM) of CTL and KO mice: sham-operated (SHAM);
426 without (BDL-) and with (BDL+) ascites (B). A Bonferroni's post test showed that the BDL+ groups (CTL or
427 KO) are significantly different from their respective SHAM groups ($p < 0.0001$ in both cases); the difference
428 between SHAM and BDL- group is not significant.

429

430 **Fig. 4**

431 αENaC abundance. Membrane protein extracts from whole kidneys from CTL (n=4) and KO (n=4) mice were
432 loaded on a single 10% polyacrylamide gel (A) and quantified. 2-way ANOVA with health status (Healthy mice,
433 SHAM, without ascites, BDL- and with ascites, BDL+) and genotype as factors, followed by Bonferroni's post-
434 test revealed significant differences (*) in the abundance of the total αENaC protein (B): KO SHAM vs KO
435 BDL+, $p < 0.0001$; KO BDL- vs KO BDL+, $p = 0.0017$; CTL BDL+ vs KO BDL+ $p = 0.0096$; for the
436 abundance of the full αENaC protein: CTL SHAM vs CTL BDL-, $p = 0.0107$ (C); KO SHAM vs KO BDL-, $p =$
437 0.0498; KO SHAM vs KO BDL+, $p = 0.0025$; and in the αENaC cleaved protein (D): KO SHAM vs KO BDL-,
438 $p = 0.0005$; KO SHAM vs KO BDL+, $p = 0.0014$; CTL BDL+ vs KO BDL+, $p = 0.018$. A 2-way ANOVA
439 revealed a significant difference for scnn1a abundance between SHAM and BDL+ ($p = 0.0133$), but neither the
440 genotype nor the interaction were significant (E).

441

442 **Fig. 5**

443 βENaC abundance. Membrane protein extracts from whole kidneys from CTL (n=4) and KO (n=4) mice were
444 loaded on a single 10% polyacrylamide gel (A) and quantified (B). 2-way ANOVA with health status (Healthy

445 mice, SHAM, without ascites, BDL- and with ascites, BDL+) and genotype as factors, followed by Bonferroni's
446 post-test revealed significant differences (*) in the abundance of the βENaC protein (B): KO SHAM vs KO
447 BDL-, $p < 0.0003$; KO BDL- vs KO BDL+, $p = 0.0001$; CTL BDL- vs KO BDL- $p = 0.0375$ (B). A 2-way
448 ANOVA revealed a significant difference for scnn1b abundance between SHAM and BDL+ ($p = 0.0185$), but
449 neither the genotype nor the interaction were significant (C).
450
451 **Fig. 6**
452 γENaC abundance. Membrane protein extracts from whole kidneys CTL (n=4) of and KO (n=4) of mice were
453 loaded on two different 4-20% polyacrylamide gels (A). Since samples from CTL and KO were not loaded on
454 the same gel, only a 1-way ANOVA was possible: No differences were seen in the total γENaC protein (full and
455 cleaved) (B); Significant differences were revealed for the abundance of the full γENaC protein: CTL BDL- vs
456 CTL BDL+, adj. $p = 0.0134$; KO BDL- vs KO BDL+, adj. $p = 0.0243$ (C); and in the γENaC cleaved protein
457 (D): CTL BDL- vs CTL BDL+, adj. $p = 0.044$; KO BDL- vs KO BDL+, adj. $p = 0.0098$. A 2-way ANOVA
458 revealed a significant difference for scnn1a abundance between SHAM and BDL+ ($p = 0.0133$), but neither the
459 genotype nor the interaction were significant (E).
460
461 **Fig. 7**
462 Na,K-ATPase abundance in cortical collecting ducts. Na,K-ATPase abundance was quantified by measuring the
463 Na,K-ATPase activity at V_{max} in microdissected CCDs from CTL and collecting ducts specific αENaC KO mice
464 for the 3 groups: SHAM-operated, without ascites (BDL-) and with (BDL+). Values represent the means ± SEM
465 from 3 to 7 mice. The number into the columns represents the n.
466
467 **Fig. 8**
468 NCC abundance: Comparison between SHAM, BDL- and BDL+. Membrane protein extracts from whole
469 kidneys of CTL and KO were loaded on a 10% polyacrylamide gel (A) and quantified (B). Since samples from
470 CTL and KO were not loaded on the same gel, only a 1-way ANOVA was possible: Significant differences were
471 revealed for the abundance of NCC in the KO group: SHAM vs BDL-, $p = 0.0287$ and BDL- vs BDL+, $p =$
472 0.0075. No difference in the relative sl12a3 (NCC) abundance (C).
473
474 **Fig. 9**
475 NCC abundance: Comparison between CTL and KO. Membrane protein extracts from whole kidneys SHAM,
476 BDL- and BDL+ were loaded on a 10% polyacrylamide gel (A) and quantified (B). Significant differences were
477 revealed for the abundance of NCC in cirrhotic mice, by Student t-test followed by Mann-Whitney post-test:
478 CTL BDL- vs KO BDL-, $p < 0.01$ and CTL BDL+ vs KO BDL+, $p < 0.01$.

FIGURE 1

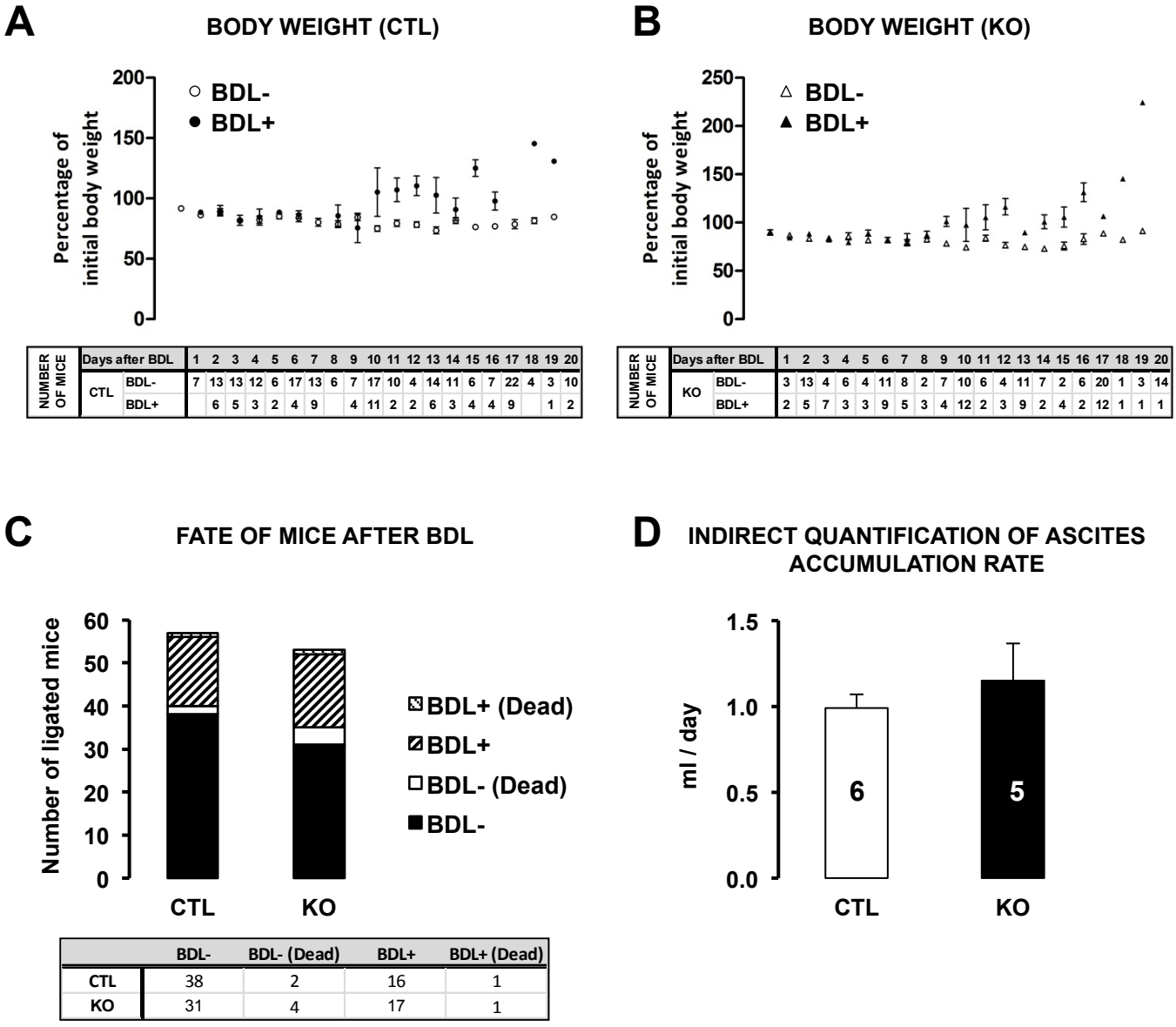

NUMBER OF MICE	Days after BDL	1	2	3	4	5	6	7	8	9	10	11	12	13	14	15	16	17	18	19	20
CTL	BDL-	7	13	13	12	6	17	13	6	7	17	10	4	14	11	6	7	22	4	3	10
	BDL+		6	5	3	2	4	9		4	11	2	2	6	3	4	4	9		1	2

NUMBER OF MICE	Days after BDL	1	2	3	4	5	6	7	8	9	10	11	12	13	14	15	16	17	18	19	20
KO	BDL-	3	13	4	6	4	11	8	2	7	10	6	4	11	7	2	6	20	1	3	14
	BDL+	2	5	7	3	3	9	5	3	4	12	2	3	9	2	4	2	12	1	1	1

	BDL-	BDL- (Dead)	BDL+	BDL+ (Dead)
CTL	38	2	16	1
KO	31	4	17	1

FIGURE 2

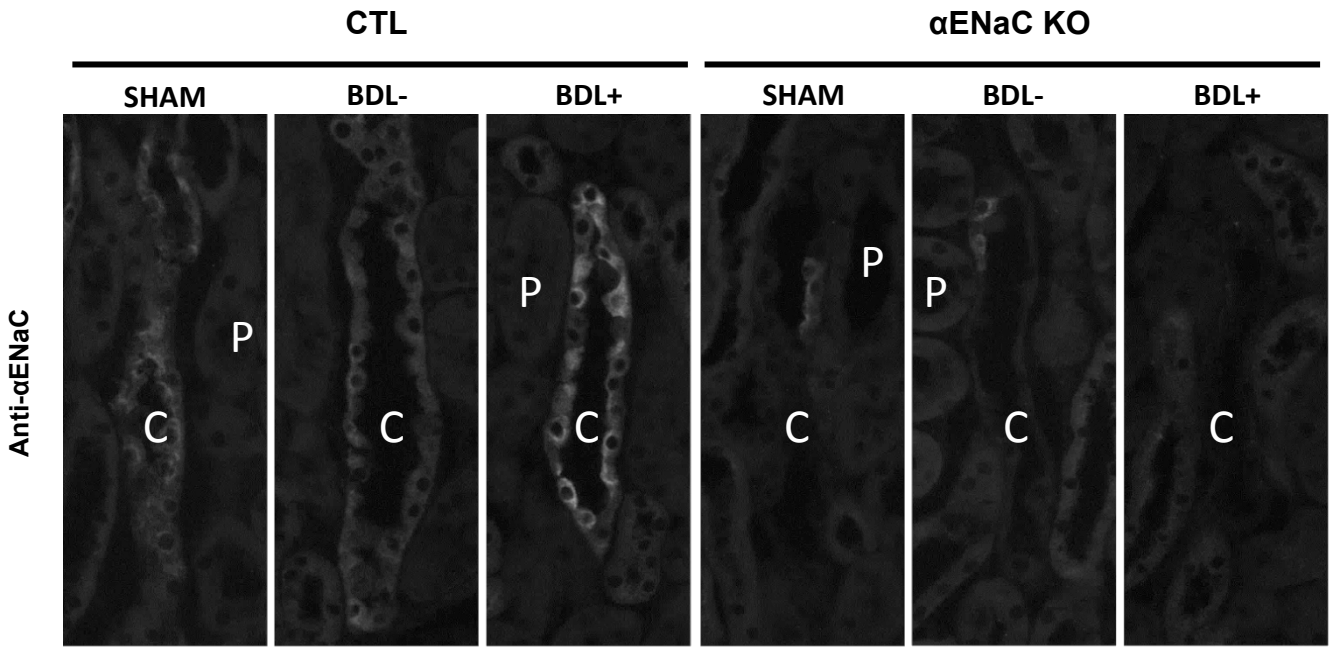
CTL
αENaC KO
SHAM
BDL-
BDL+
SHAM
BDL-
BDL+
Anti-αENaC
P
C
P
C
P
C
P
C
P
C
C

FIGURE 3

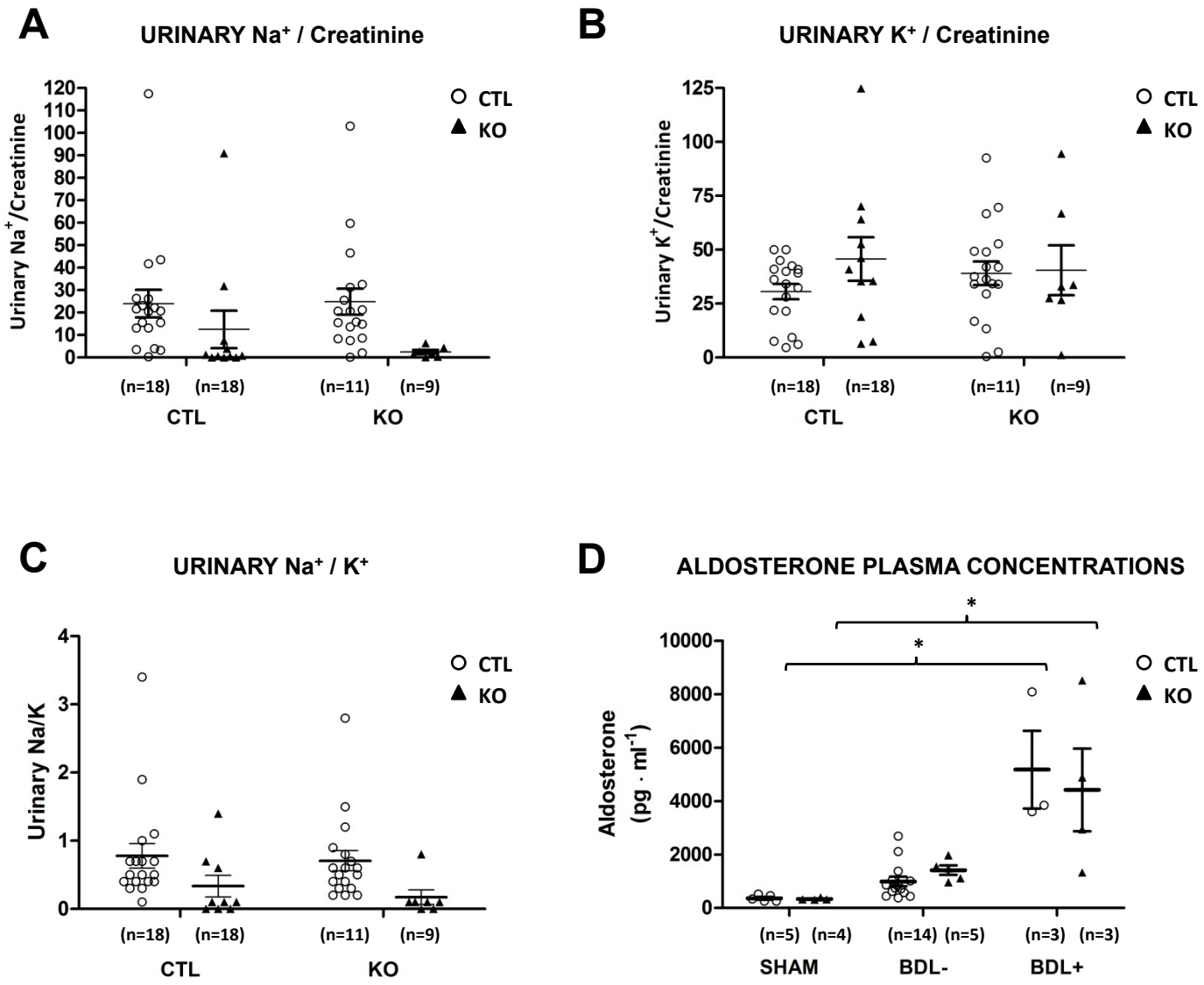
A
URINARY Na+ / Creatinine
Urinary Na+/Creatinine
120
110
100
90
80
70
60
50
40
30
20
10
0
CTL
KO
(n=18)
(n=18)
(n=11)
(n=9)
CTL
KO
B
URINARY K+ / Creatinine
Urinary K+/Creatinine
125
100
75
50
25
0
CTL
KO
(n=18)
(n=18)
(n=11)
(n=9)
CTL
KO
C
URINARY Na+ / K+
Urinary Na/K
4
3
2
1
0
CTL
KO
(n=18)
(n=18)
(n=11)
(n=9)
CTL
KO
D
ALDOSTERONE PLASMA CONCENTRATIONS
Aldosterone (pg · ml-1)
10000
8000
6000
4000
2000
0
*
*
CTL
KO
(n=5)
(n=4)
(n=14)
(n=5)
(n=3)
(n=3)
SHAM
BDL-
BDL+

FIGURE 4

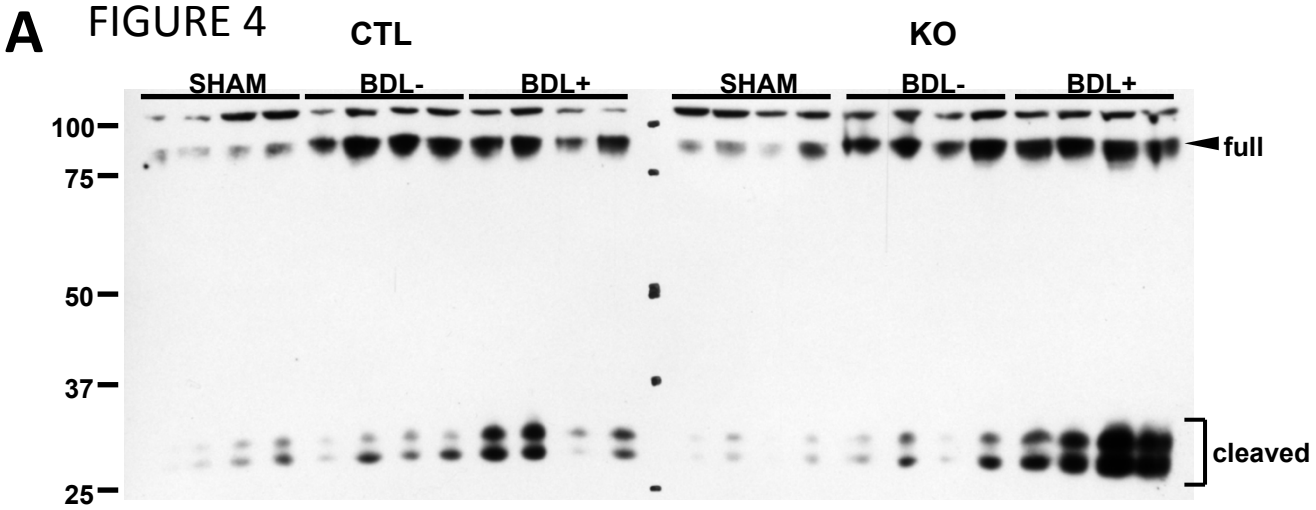
A
CTL
KO
SHAM
BDL-
BDL+
SHAM
BDL-
BDL+
100
75
50
37
25
full
cleaved

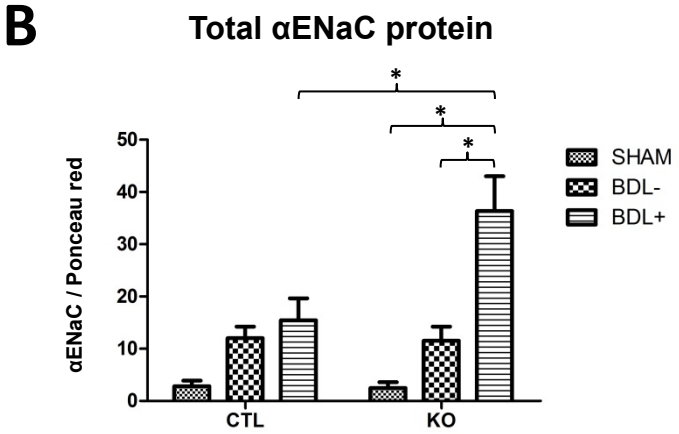
B
Total αENaC protein
αENaC / Ponceau red
50
40
30
20
10
0
CTL
KO
SHAM
BDL-
BDL+
*
*
*

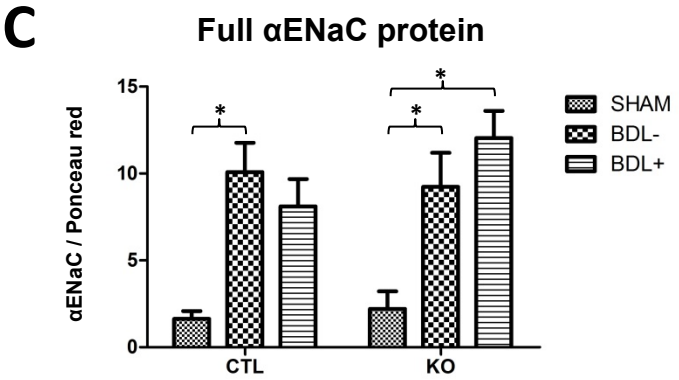
C
Full αENaC protein
αENaC / Ponceau red
15
10
5
0
CTL
KO
SHAM
BDL-
BDL+
*
*
*

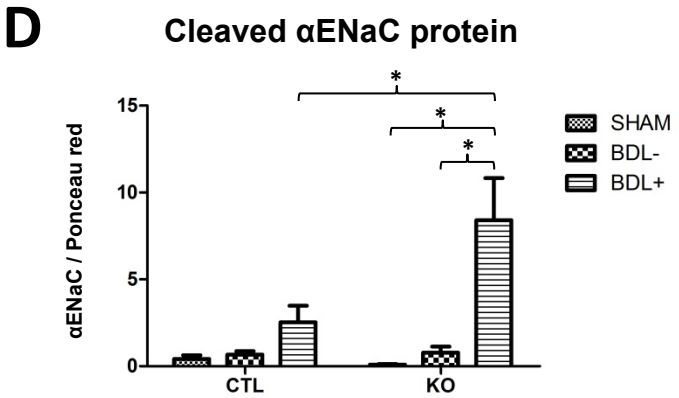
D
Cleaved αENaC protein
αENaC / Ponceau red
15
10
5
0
CTL
KO
SHAM
BDL-
BDL+
*
*
*

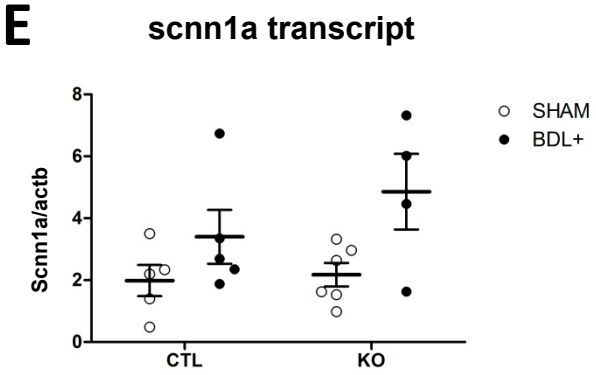
E
scnn1a transcript
Scnn1a/actb
8
6
4
2
0
CTL
KO
SHAM
BDL+

FIGURE 5

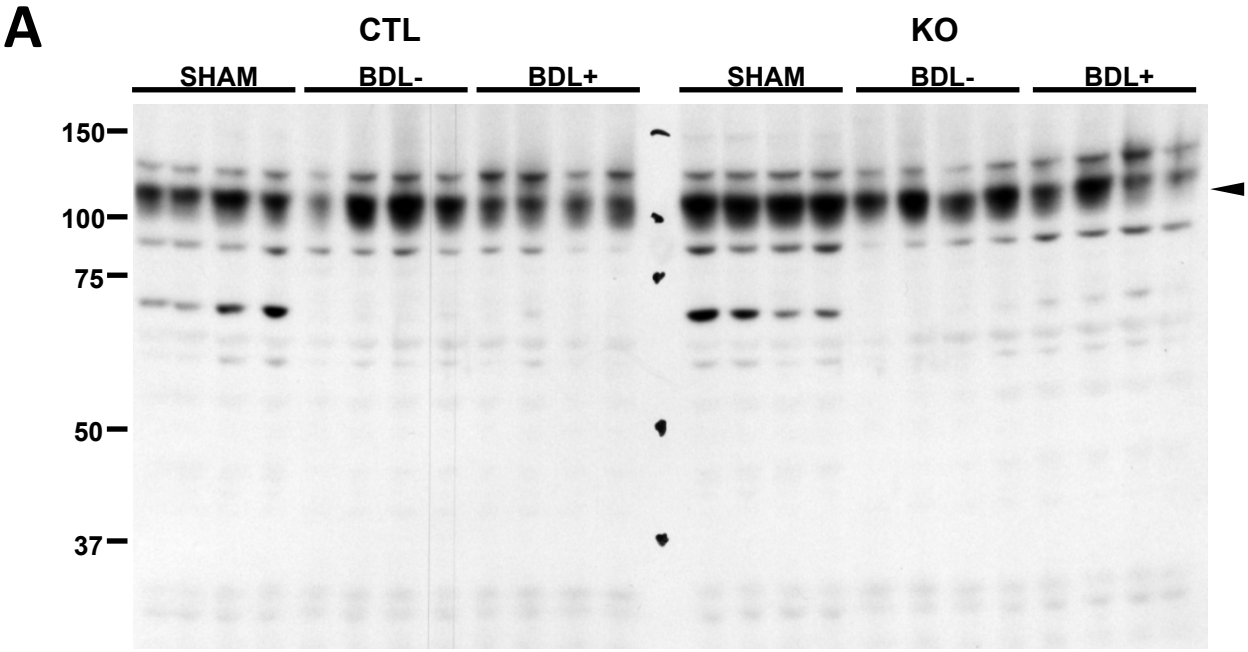
A
CTL
KO
SHAM
BDL-
BDL+
SHAM
BDL-
BDL+
150
100
75
50
37

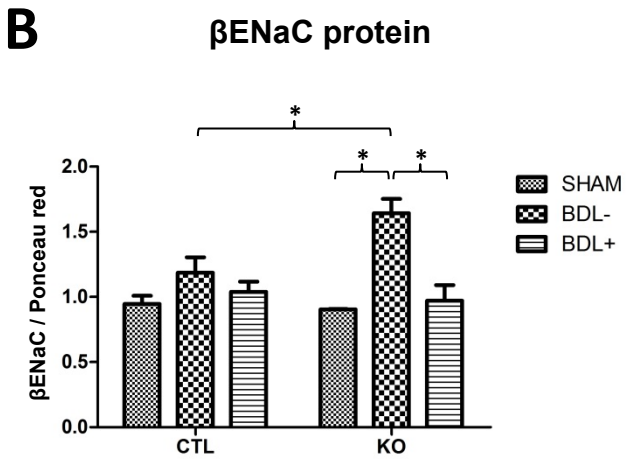
B
βENaC protein
βENaC / Ponceau red
2.0
1.5
1.0
0.5
0.0
CTL
KO
SHAM
BDL-
BDL+
*
*
*

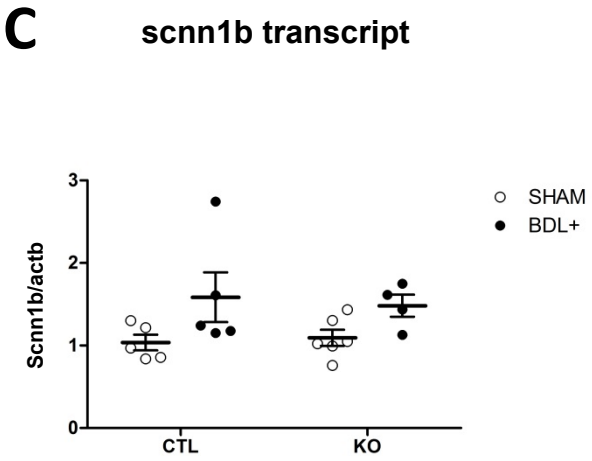
C
scnn1b transcript
Scnn1b/actb
3
2
1
0
CTL
KO
SHAM
BDL+

FIGURE 6

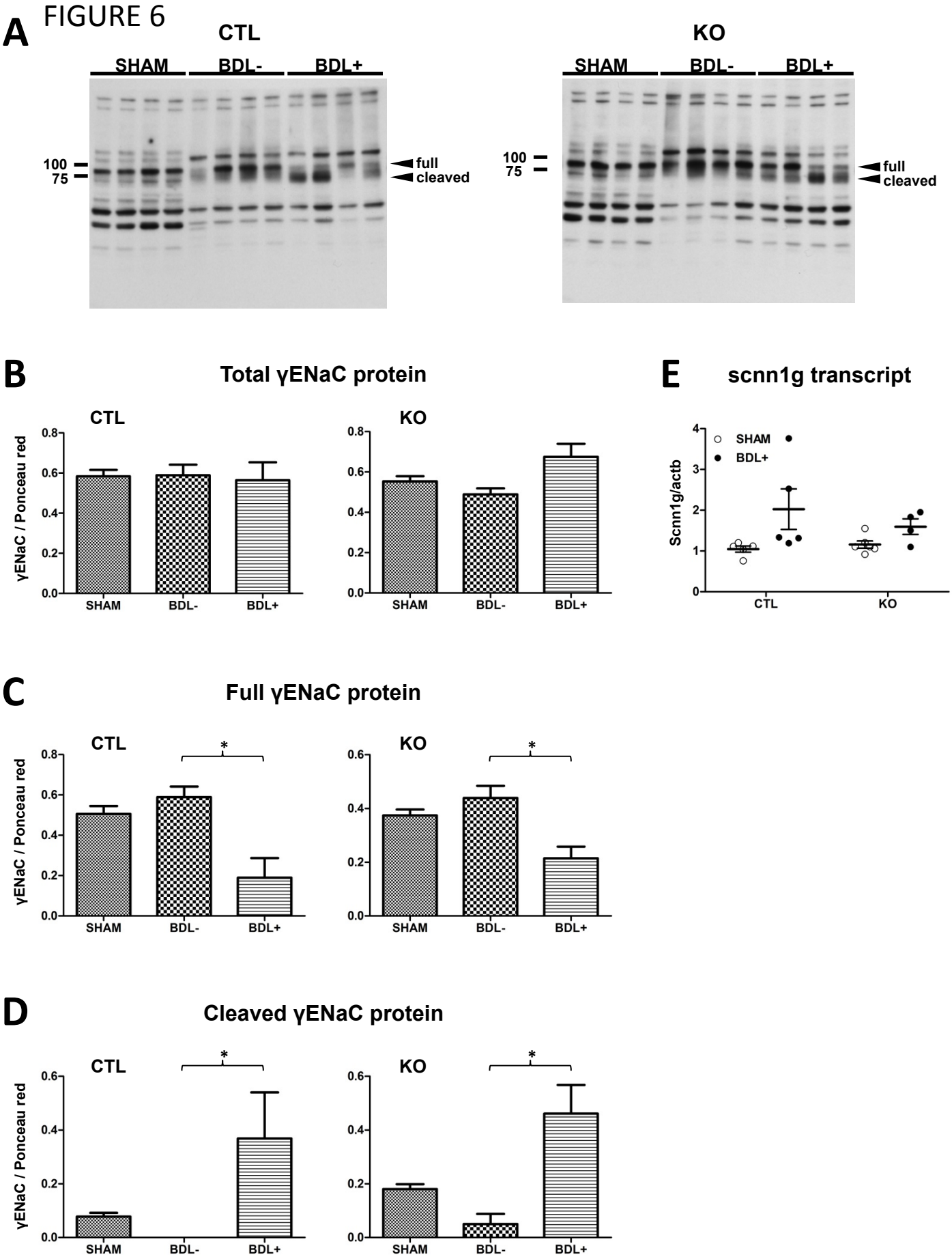
A
CTL
SHAM
BDL-
BDL+
100
75
full
cleaved
KO
SHAM
BDL-
BDL+
100
75
full
cleaved
B
Total γENaC protein
CTL
KO
γENaC / Ponceau red
0.0
0.2
0.4
0.6
0.8
SHAM
BDL-
BDL+
E
scnn1g transcript
SHAM
BDL+
Scnn1g/actb
0
1
2
3
4
CTL
KO
C
Full γENaC protein
CTL
KO
*
γENaC / Ponceau red
0.0
0.2
0.4
0.6
0.8
SHAM
BDL-
BDL+
D
Cleaved γENaC protein
CTL
KO
*
γENaC / Ponceau red
0.0
0.2
0.4
0.6
SHAM
BDL-
BDL+

FIGURE 7

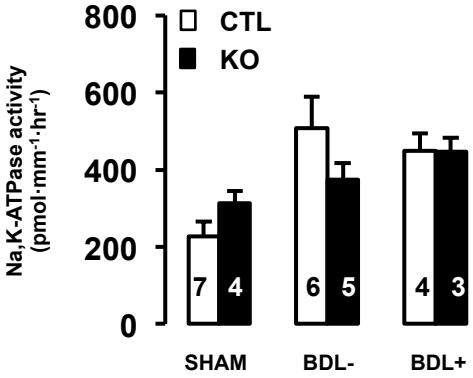
800
600
400
200
0
CTL
KO
Na,K-ATPase activity
(pmol·mm-1·hr-1)
7
4
6
5
4
3
SHAM
BDL-
BDL+

FIGURE 8

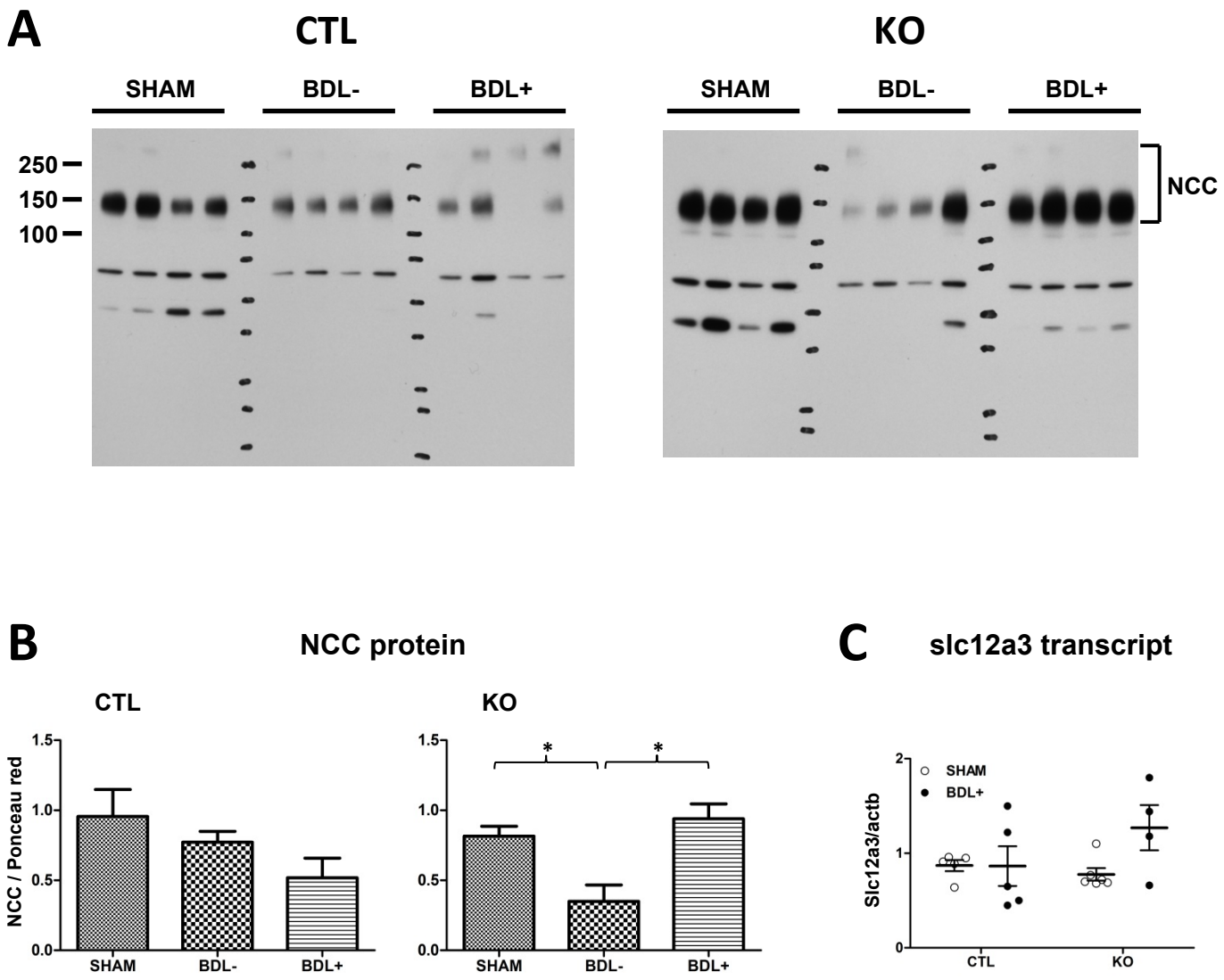
A
CTL
KO
SHAM
BDL-
BDL+
SHAM
BDL-
BDL+
250
150
100
NCC
B
NCC protein
CTL
KO
NCC / Ponceau red
1.5
1.0
0.5
0.0
SHAM
BDL-
BDL+
*
*
C
slc12a3 transcript
Slc12a3/actb
2
1
0
SHAM
BDL+
CTL
KO

FIGURE 9

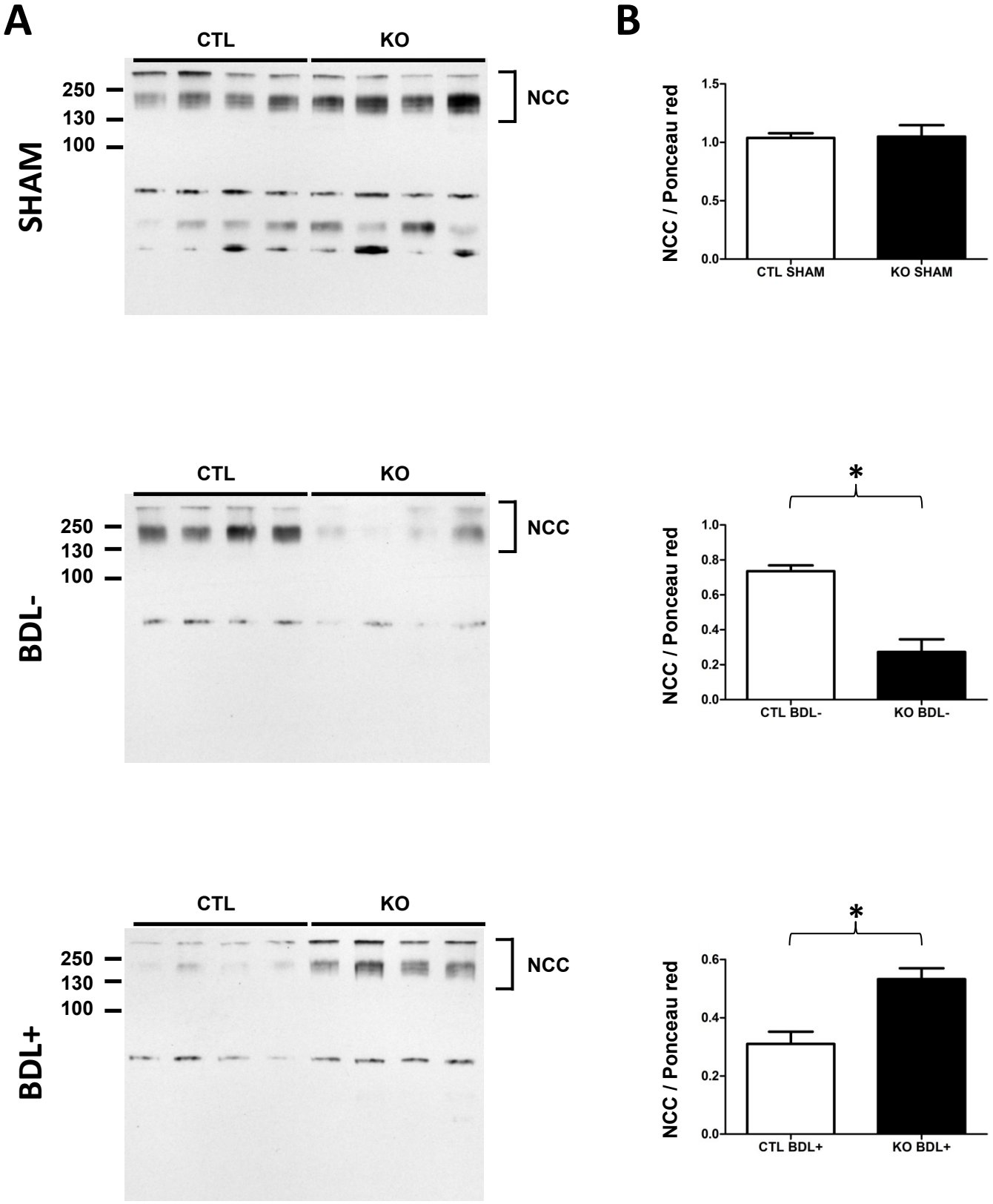
A
B
CTL
KO
250
130
100
NCC
SHAM
BDL-
BDL+
NCC / Ponceau red
1.5
1.0
0.5
0.0
CTL SHAM
KO SHAM
0.8
0.6
0.4
0.2
CTL BDL-
KO BDL-
*
CTL BDL+
KO BDL+